Superimposed Asymmetric Modulation in Narrowband Fading Channels using Orthogonal Codes

S. W. L. Poon, *Member, IEEE,* K. N. Plataniotis, *Senior Member, IEEE,* and S. Pasupathy, *Fellow, IEEE*

Abstract— The asymmetric signal constellation (ASC) method to break isometry is analyzed in a superimposed symbol framework with a Kalman filter estimator (KF) / maximum-likelihood (ML) detector as the receiver. Direct application of the ASC method led to a bit error floor, which motivates the proposal of combining orthogonal spreading codes with ASC to solve this problem. The proposed scheme generalizes previously proposed ASC and pilot-assisted solutions in a systematic way and results in coherent detection schemes without set bit error floors and better performance.

Index Terms— Asymmetric modulation, Superimposed, Orthogonal codes, Pilot symbols, Coherent, Kalman filter, Gauss-Markov, Maximum likelihood detection.

I. INTRODUCTION

THE main objective of a communications receiver is to detect data sent from the transmitter with minimal error probability. Data detection can be performed coherently or non-coherently. Coherent detection requires channel estimation, but it results in better probability of error performance than non-coherent detection. This letter focuses on coherent detection of phase-shift keying (PSK) signals in a narrowband flat fading channel. In such a scenario, the transmitted signal is distorted by additive white Gaussian noise (AWGN) and multiplicative fading [1]–[3]. Joint channel estimation / data detection (CE/DD) systems suffer from irreducible error floors as a result of the combined effects of erroneous data detection and large estimation errors [1]. It was shown in [4] that the cause is isometry, which can be defined as ambiguity in detecting the correct data symbol that arises from multiplicative channel fading effects and rotational invariance of PSK constellations. One solution to this problem is time-division-multiplexed (TDM) pilot-assisted transmission (PAT) in which detection ambiguity is eliminated at the receiver. The term PAT refers to general transmission schemes that use pilot symbols to aid the process of channel estimation [5]. It is different from pilot symbol-assisted modulation (PSAM) [6] in that PSAM specifically refers to PAT with regular periodic placement of cluster size 1 (RPP-1) [5].

An alternative to TDM PAT is superimposed PAT, where part of the power in each data symbol is allocated to a parallel pilot channel to transmit known symbols. Fig. 1A shows the symbol structure of superimposed PAT. The pilot channel provides a continuous stream of pilot symbols to enable the
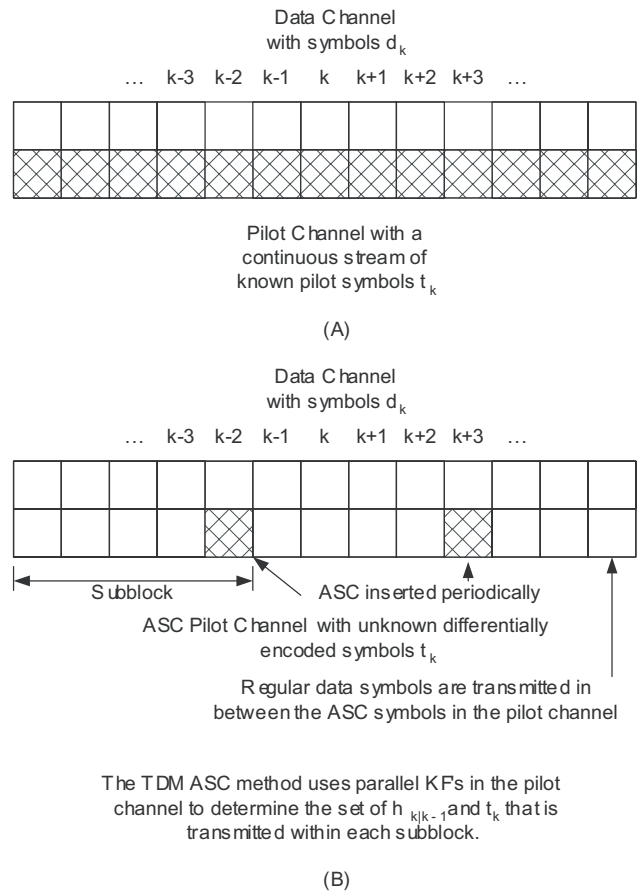
Fig. 1. (A) Symbol structure of the superimposed PAT. (B) Symbol structure of the NS-ASC.

estimator to update its channel estimate while user data is transmitted in a separate parallel data channel. Superimposed PAT is considered in this letter because it outperforms the optimal TDM PAT scheme, the RPP-1 TDM PAT, in bit error rate (BER) and minimum mean square error (MMSE) for the majority of fading rates of practical importance [5].

At the receiver, the continuous-time received signal is matched filtered (MF) and sampled at symbol rate to obtain the sufficient statistics. The first column of Table I shows equations and statistics for the discrete-time received signal in the kth symbol interval and the receiver that is used for this scheme. In the table, ρ_t^2 and ρ_d^2 are the powers allocated to pilot and data symbols respectively, $\{t_k\}$ and $\{d_k\}$ are the pilot and data sequences respectively, h_k is the fading channel coefficient, and w_k is AWGN. A first-order Gauss-Markov process expressed in state space form is used to model the dynamics of the channel state h_k due to its reasonable complexity

TABLE I
RECEIVER MODEL COMPARISON OF THE THREE SUPERIMPOSED SCHEMES

	Superimposed PAT	NS-ASC	OS-ASC
Rx Signal	$y_k = \rho_t t_k h_k + \rho_d d_k h_k + w_k$	$y_k = \rho_t t_k h_k + \rho_d d_k h_k + w_k$	$\mathbf{r}_k = SA_k \mathbf{b}_k + \mathbf{w}_k$
Received Signal Statistics	$h_k \sim \mathcal{CN}(0, \sigma_h^2)$ $w_k \overset{i.i.d}{\sim} \mathcal{CN}(0, \sigma_w^2)$ $E[t_k] = E[d_k] = 0$ $E[\,\|t_k\|^2] = E[\,\|d_k\|^2] = 1$ $\{t_k\}, \{d_k\}$ are iid PSK symbols	$h_k \sim \mathcal{CN}(0, \sigma_h^2)$ $w_k \overset{i.i.d}{\sim} \mathcal{CN}(0, \sigma_w^2)$ $E[t_k] = E[d_k] = 0$ $E[\,\|t_k\|^2] = E[\,\|d_k\|^2] = 1$ $\{t_k\}, \{d_k\}$ are iid PSK symbols	$S = [\mathbf{s}_t\ \mathbf{s}_d], S^H S = R = I$ $A_k = h_k I, \mathbf{b}_k = [\rho_t t_k\ \rho_d d_k]^T$ $E[\mathbf{w}(k)] = \mathbf{0}$ $E[\mathbf{w}_k \mathbf{w}_{k+m}^*] = \sigma_w^2 I \delta(m)$ $\{t_k\}, \{d_k\}$ are iid PSK symbols
Correlator Output and Statistics	Not Applicable	Not Applicable	$\mathbf{y}_k = S^H \mathbf{r}_k = A_k \mathbf{b}_k + \mathbf{q}_k$ $\mathbf{y}_k = [y_{tk}\ y_{dk}]^T$ $\mathbf{q}_k = S^H \mathbf{w}_k, E[\mathbf{q}(k)] = \mathbf{0}$ $E[\mathbf{q}_k \mathbf{q}_{k+m}^*] = \sigma_w^2 I \delta(m)$
Channel Hypermodel	$h_k = a h_{k-1} + u_k$ $u_k \overset{i.i.d}{\sim} \mathcal{CN}(0, (1-a^2)\sigma_h^2)$	$h_k = a h_{k-1} + u_k$ $u_k \overset{i.i.d}{\sim} \mathcal{CN}(0, (1-a^2)\sigma_h^2)$	$h_k = a h_{k-1} + u_k$ $u_k \overset{i.i.d}{\sim} \mathcal{CN}(0, (1-a^2)\sigma_h^2)$
Pilot Channel Receiver	KF to obtain $\hat{h}_{k|k}$ $\{t_k\}$ known, detection unnecessary	Coupled KF/ML CE/DD to obtain $\hat{h}_{k|k}$ and $\hat{t}_k$ (TDM ASC method) [4]	Coupled KF/ML CE/DD to obtain $\hat{h}_{k|k}$ and $\hat{t}_k$ (TDM ASC method) [4]
Data Rxer	ML detector to obtain $\hat{d}_k$	ML detector to obtain $\hat{d}_k$	ML detector to obtain $\hat{d}_k$
Meas. Eqn.	$y_k = \rho_t t_k h_k + v_k$	$y_k = \rho_t t_k h_k + v_k$	$y_{tk} = \rho_t t_k h_k + \mathbf{s}_t^H \mathbf{w}_k$
Meas. Equation Statistics	$v_k = \rho_d d_k h_k + w_k$ $E[v_i v_j^*] = \sigma_v^2 \delta_{ij}, E[h_i v_j^*] = 0$ $\sigma_v^2 = (\rho_d^2 \sigma_h^2 + \sigma_w^2)$	$v_k = \rho_d d_k h_k + w_k$ $E[v_i v_j^*] = \sigma_v^2 \delta_{ij}, E[h_i v_j^*] = 0$ $\sigma_v^2 = (\rho_d^2 \sigma_h^2 + \sigma_w^2)$	$E[\mathbf{s}_t^H \mathbf{w}_k] = 0$ $E[(\mathbf{s}_t^H \mathbf{w}_k)(\mathbf{s}_t^H \mathbf{w}_k)^H] = \sigma_w^2$
KF Recursive Equations	$\hat{h}_{k|k-1} = a\hat{h}_{k-1|k-1}, \hat{h}_{0|0} = 0$ $P_{k|k-1} = a^2 P_{k-1|k-1} + (1-a^2)\sigma_h^2,$ $P_{0|0} = 1$ $z_{k|k-1} = y_k - \rho_t t_k \hat{h}_{k|k-1}$ $P_{z\,k|k-1} = \rho_t^2 P_{k|k-1} + (\rho_d^2 \sigma_h^2 + \sigma_w^2)$ $K_k = P_{k|k-1}(\rho_t t_k)^H P_{z\,k|k-1}^{-1}$ $\hat{h}_{k|k} = \hat{h}_{k|k-1} + K_k z_{k|k-1}$ $P_{k|k} = [1 - K_k(\rho_t t_k)]P_{k|k-1}$	$\hat{h}_{k|k-1} = a\hat{h}_{k-1|k-1}, \hat{h}_{0|0} = 0$ $P_{k|k-1} = a^2 P_{k-1|k-1} + (1-a^2)\sigma_h^2,$ $P_{0|0} = 1$ $z_{k|k-1} = y_k - \rho_t t_k \hat{h}_{k|k-1}$ $P_{z\,k|k-1} = \rho_t^2 P_{k|k-1} + (\rho_d^2 \sigma_h^2 + \sigma_w^2)$ $K_k = P_{k|k-1}(\rho_t t_k)^H P_{z\,k|k-1}^{-1}$ $\hat{h}_{k|k} = \hat{h}_k = \hat{h}_{k|k-1} + K_k z_{k|k-1}$ $P_{k|k} = [1 - K_k(\rho_t t_k)]P_{k|k-1}$	$\hat{h}_{k|k-1} = a\hat{h}_{k-1|k-1}, \hat{h}_{0|0} = 0$ $P_{k|k-1} = a^2 P_{k-1|k-1} + (1-a^2)\sigma_h^2,$ $P_{0|0} = 1$ $z_{k|k-1} = y_{tk} - \rho_t t_k \hat{h}_{k|k-1}$ $P_{z\,k|k-1} = \rho_t^2 P_{k|k-1} + \sigma_w^2$ $K_k = P_{k|k-1}(\rho_t t_k)^H P_{z\,k|k-1}^{-1}$ $\hat{h}_{k|k} = \hat{h}_k = \hat{h}_{k|k-1} + K_k z_{k|k-1}$ $P_{k|k} = [1 - K_k(\rho_t t_k)]P_{k|k-1}$
Pilot and Data Chan. Detectors	t_k known, no detection required $\hat{d}_k = \underset{d_k \in D_k}{\arg\min}$ $\|(y_k - \rho_t t_k \hat{h}_{k|k}) - \rho_d d_k \hat{h}_{k|k}\|^2$ [5]	$\hat{t}_k = \underset{t_k \in T_k}{\arg\min} \|y_k - \rho_t t_k \hat{h}_{k|k-1}\|^2$ $\hat{d}_k = \underset{d_k \in D_k}{\arg\min}$ $\|(y_k - \rho_t \hat{t}_k \hat{h}_{k|k}) - \rho_d d_k \hat{h}_{k|k}\|^2$ [5]	$\hat{t}_k = \underset{t_k \in T_k}{\arg\min} \|y_{tk} - \rho_t t_k \hat{h}_{k|k-1}\|^2$ $\hat{d}_k = \underset{d_k \in D_k}{\arg\min}$ $\|y_{dk} - \rho_d d_k \hat{h}_{k|k}\|^2$
Dat. Chan. Observation and Stats	$y'_k = y_k - \rho_t t_k \hat{h}_{k|k}$	$y'_k = y_k - \rho_t \hat{t}_k \hat{h}_{k|k}$	$y'_k = y_{dk} = \rho_d d_k h_k + \mathbf{s}_d^H \mathbf{w}_k$ $E[\mathbf{s}_d^H \mathbf{w}_k] = 0$ $E[(\mathbf{s}_d^H \mathbf{w}_k)(\mathbf{s}_d^H \mathbf{w}_k)^H] = \sigma_w^2$

and good performance in approximating a Rayleigh fading power spectral density (PSD) [2]. When no prior information is available about the dynamics of h_k, $a \in [0.9 - 0.99]$ is often a reasonable and robust choice for this hypermodel [2]. A small a represents fast fading while a large a represents slow fading. The standard conditions in [5] assume that t_k, d_k, h_k, and w_k are jointly independent.

A joint CE/DD receiver consisting of a Kalman filter (KF) and a maximum-likelihood (ML) detector was proposed in [5] for the superimposed PAT. The KF operates in the pilot channel and it considers the term $\rho_d d_k h_k$ in y_k in the first column of Table I as noise-like interference that is grouped with the AWGN w_k to create the term v_k in the measurement equation. As KF is a recursive estimator, the channel

initial conditions need to be known. In the absence of prior information, the channel estimate $\hat{h}_{0|0} = 0$ and the estimation covariance $P_{0|0} = 1$ are used to match the statistical conditions of a Rayleigh fading channel [2], [4]. The ML detector selects the data sequence $\{d_k\}$ based on the criterion in Table I and derived in Appendix I.

The disadvantages of both TDM and superimposed PAT are that they reduce effective data transmission rate and consume extra transmission power. Recently, a method that involves the periodic TDM of asymmetric signal constellations (ASC) was proposed in [4] to break isometry using a decision-directed KF/ML joint CE/DD. Under this receiver model, TDM ASC achieves similar mean square error (MSE) and bit error rate (BER) performance as TDM PAT [4]. Hence, this method has

the potential to replace TDM PAT because it does not use any pilot symbols. Note that the KF for TDM PAT in [5] relies solely on the first-order Gauss-Markov hypermodel to update $\hat{h}_{k|k}$ and $P_{k|k}$ at non-pilot points (Hypermodel TDM PAT). This is different from the KF in [4] where it operates in decision-directed mode for every symbol in the frame (Decision-directed TDM PAT). Nonetheless, a Hypermodel TDM ASC scheme could similarly be set up by replacing the pilot symbol time slots in Hypermodel TDM PAT with ASCs and by using the receiver model in [5]. It was shown in [5] that superimposed PAT outperforms the Hypermodel TDM PAT. Thus, let us device and analyze a superimposed ASC scheme that could be used to similarly replace superimposed PAT.

The main contribution of this letter is to present a generalized framework for the cost effective solution to the problem of joint CE/DD in narrowband channels. This includes: (i) the discussion and analysis of a naïve superimposed ASC scheme based on the application of the techniques in [4], (ii) the discovery of an error floor in this scheme due to a bounded signal-to-interference plus noise ratio (SINR), (iii) the proposal of an orthogonal code superimposed ASC scheme that removes the error floor, and provides better BER performance than superimposed PAT.

II. THE NAÏVE SUPERIMPOSED ASC (NS-ASC) SCHEME

The NS-ASC scheme is a direct application of the TDM ASC method in [4] to the superimposed PAT framework in [5]. The second column in Table I shows the equations for the received signal and the NS-ASC receiver. Since the superimposed PAT framework is used, columns one and two in table I are very similar. The difference is that t_k needs to be detected as all pilot symbols in the pilot channel are replaced by unknown data symbols. The joint ignorance of both h_k and t_k in the pilot channel results in isometry. Isometry can be illustrated as follows: Suppose the t_k constellation $T_k = e^{j\frac{2\pi m}{M}} t_k$, $m = 0, 1, \cdots, M-1$ is regular M-PSK. Based on the initial condition $\hat{h}_{0|0} = 0$, all M points in T_1 minimize the detection criterion for t_k in Table I, hence the term isometry. Assuming that t_1 is transmitted and v_1 is negligible in the measurement equation, an incorrect choice of $\hat{t}_1 = e^{j\frac{2\pi m}{M}} t_1$, $m \neq 0$ would result in an incorrect channel estimate $\hat{h}_{1|1} = e^{-j\frac{2\pi m}{M}} h_1$. It was shown in [4] that the coupled KF/ML CE/DD system for the NS-ASC scheme propagates rotational invariance. Therefore, for $k = 2, 3, \cdots$, $\hat{h}_{k|k} = e^{-j\frac{2\pi m}{M}} h_k$ instead of h_k. The decision rule for t_k would select $\hat{t}_k = e^{j\frac{2\pi m}{M}} t_k$ over t_k, which leads to more estimation and detection errors in subsequent symbols. The probability of selecting an erroneous first symbol is $(1 - \frac{1}{M})$, which shows that isometry leads to an irreducible error floor.

Fig. 1B shows the symbol structure of the NS-ASC. Since the joint CE/DD structure in the pilot channel is identical to that in [4], the TDM ASC CE/DD method using parallel KF's in [4] can be used here to find a unique sequence of $\{t_k\}$ and $\{\hat{h}_{k|k}\}$. Symbols are differentially encoded and decoded (DED) to remove phase ambiguity between adjacent symbols. The differential encoding rule is $t_k = t_{k-1} c_k$, where c_k is the uncoded symbol and $t_0 = 1$, and the decoding rule
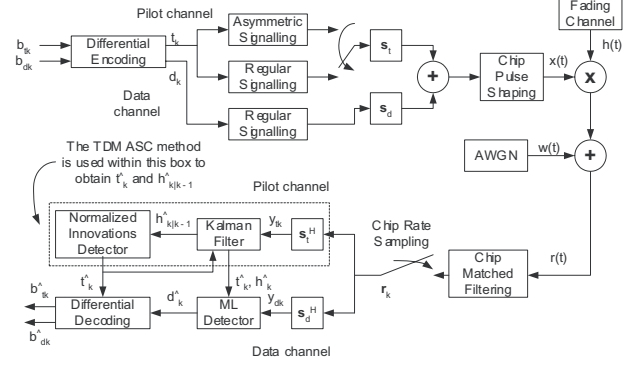

Fig. 2.   Block diagram of the OS-ASC transceiver.

is $c_k = t_k t_{k-1}^*$. ASCs are inserted periodically in between data symbols in the pilot channel to break isometry [4]. The reader is referred to [4] for further details on the mechanics of this method. The ML detection rule for t_k is derived in Appendix I while the detection rule for d_k is the same as that in superimposed PAT.

III. THE ORTHOGONAL SUPERIMPOSED ASC (OS-ASC) SCHEME

It will be shown in the next section that an error floor severely degrades the BER performance of NS-ASC and the source of this problem is the interference $\rho_d d_k h_k$ seen by the pilot channel during the detection of t_k, which is not required in superimposed PAT. In order for NS-ASC's performance to approach that of superimposed PAT, the error floor must be removed by forcing $\rho_d d_k h_k \rightarrow 0$. The solution proposed here is to spread d_k and t_k by different orthogonal codes $\mathbf{s_d}$ and $\mathbf{s_t}$ of length N such that the pilot channel becomes orthogonal to the data channel. Fig. 2 shows a block diagram of the OS-ASC transceiver structure proposed in this letter. The continuous-time signal is now a superposition of chip pulses instead of symbol pulses. Thus, the MF is matched to the chip pulse shape and sampled at the chip rate to obtain the sufficient statistics in this case. The equations for the discrete-time signal and the receiver in Fig. 2 is given in column three of Table I. $\mathbf{r}_k$ is the N x 1 received signal, S is the N x 2 spreading code matrix, A_k is a 2 x 2 channel matrix, $\mathbf{w}_k$ is a N x 1 AWGN vector, R is the spreading code correlation matrix, and $\mathbf{q}_k$ is a 2 x 1 additive noise vector.

Before $\mathbf{r}_k$ is input into the joint KF/ML CE/DD, it is correlated with S to completely remove the interference between the pilot and data channels. The interference could be completely removed because both d_k and t_k in the 2 x 1 data vector $\mathbf{b}$ undergo the same channel perturbation. As a result, $\mathbf{s_t}$ and $\mathbf{s_d}$ remain orthogonal at the receiver. Furthermore, it is important to note that $\mathbf{s_d}$ and $\mathbf{s_t}$ are both known at the receiver because all the codes belong to the same user.

The symbol structure of OS-ASC remains unchanged from NS-ASC and it can be described by Fig. 1B. According to Fig. 2, y_{tk} is passed to a joint KF/ML CE/DD in the pilot channel while y_{dk} is passed to the ML detector in the data channel. The TDM ASC method in [4] is used in the pilot channel to obtain the sequences $\{\hat{h}_{k|k}\}$ and $\{\hat{t}_k\}$. $\hat{d}_k$ is obtained symbol-

by-symbol using the decision rule given in column three of Table I. This rule is derived in Appendix I.

The tradeoff of using OS-ASC as opposed to superimposed PAT or NS-ASC is that the spreading codes enlarge the original signal's bandwidth by N times. Fortunately, orthogonal codes are able to completely remove interference with a very small N For a superimposed framework with only two channels, the smallest N that achieves this purpose is $N = 2$. Any larger N would reduce the spectral efficiency (measured in bits/s/Hz) without providing further gain in performance. If the original signal is narrowband, $\mathbf{r}_k$ can still be considered as a narrowband signal with $N = 2$.

IV. PROBABILITY OF ERROR ANALYSIS FOR THE SUPERIMPOSED SCHEMES

A. The Naïve Superimposed ASC Scheme

The total error probability is given by $P_e(k) = \frac{1}{2}P_{e,t}(k) + \frac{1}{2}P_{e,d}(k)$, where $P_{e,t}(k)$ and $P_{e,d}(k)$ are the error probabilities for t_k and d_k respectively. A closed-form expression of $P_{e,t}(k)$ is derived in Appendix II based on the t_k detection criterion given in column two of Table I. In order to check how high $P_{e,t}(k)$ gets, a lower bound analysis can be performed by setting the prediction covariance $P_{k|k-1} = 0$ in (4). Under such an assumption,

$$P_{e,t,LB}(k) \approx \frac{\mathcal{K}}{2}\left[1 - \sqrt{\frac{1}{\frac{4}{d_{min}^2}\left(\frac{1}{\beta}\right) + 1}}\right] \tag{1}$$

where β is the SINR from the KF's viewpoint, defined by

$$\beta \triangleq \frac{E[|\rho_t t_k h_k|^2]}{E[|v_k|^2]} = \frac{\sigma_h^2 \rho_t^2}{\sigma_h^2 \rho_d^2 + \sigma_w^2} = \frac{\sigma_h^2 \rho_t^2}{\sigma_v^2}. \tag{2}$$

The power is split up equally between the data and pilot channels in [5] such that $\rho_t^2 = \rho_d^2 = P/2$. To simplify matters more, let $\sigma_h^2 = 1$ for a Rayleigh fading channel and let $P = 1$. By substituting these into (2), β simplifies to $\beta = \frac{1}{1+\frac{2}{SNR}}$ where $SNR \triangleq \frac{\sigma_h^2 P}{\sigma_w^2}$. According to this β expression, β goes from 0 ($-\infty$ dB) to 1 (0 dB) as SNR goes from 0 to ∞. This means there is a BER floor according to (1). In order to see where this BER floor resides, let us examine a scenario where t_k is a BPSK signal. For BPSK, $\mathcal{K} = 1$ and $d_{min} = 2$. Therefore, the lower bound of $P_{e,t}(k)$ is $P_{e,t,LB,BPSK}(k) = \frac{1}{2}\left[1 - \sqrt{\frac{1}{1+\frac{1}{\beta}}}\right]$. By substituting $\beta = 1$ for minimum BER, $P_{e,t,LB,BPSK}(k) = 0.146$. For other PSK constellations where $d_{min} < 2$ and $\mathcal{K} > 1$, $P_{e,t,LB}(k) \geq 0.146$.

In joint CE/DD receivers, MSE and BER are coupled together. A high BER floor in t_k would also result in inaccurate $\hat{h}_{k|k}$ and a large $P_{k|k}$ from the KF. Since Table I shows that the data channel uses $\hat{h}_{k|k}$ to form the detection criterion for d_k, a high MSE in $\hat{h}_{k|k}$ would create a high $P_{e,d}(k)$. Therefore, $P_{e,d}(k)$ should be similar to $P_{e,t}(k)$, which would render NS-ASC unusable for reliable transmission.

Although superimposed PAT also sees the same SINR in the pilot channel, it does not have a BER floor because t_k does not need to be detected. According to the P_e expression (29) in [5], $P_e(k) = P_{e,d}(k) \to 0$ as $\beta \to 1$ [5]. The analysis in

this subsection indicates that an error floor exists for NS-ASC and the source behind this is the interference term $\rho_d d_k h_k$.

B. The Orthogonal Superimposed ASC Scheme

With $\mathbf{s}_d$ and $\mathbf{s}_t$ removing the interference in the pilot channel, $\sigma_v^2 = \sigma_w^2$ and $\beta = \frac{\rho_t^2 \sigma_h^2}{\sigma_w^2} \triangleq SNR_t$. Since $\rho_t^2 \propto P$, $SNR_t \propto SNR$. The detection rule for t_k in this scenario is the same as NS-ASC. Thus, the probability of error is given by

$$P_{e,t}(k) \approx \frac{\mathcal{K}}{2}\left[1 - \sqrt{\frac{1 - \frac{P_{k|k-1}}{\sigma_h^2}}{\left(\frac{4}{d_{min}^2} - 1\right)\frac{P_{k|k-1}}{\sigma_h^2} + \frac{4}{d_{min}^2}\left(\frac{1}{SNR_t}\right) + 1}}\right]$$

(Appendix II).

Notice that the $\frac{1}{\beta}$ term in (4) is changed to $\frac{1}{SNR_t}$ here and $SNR_t \to \infty$ as $SNR \to \infty$. Thus, $P_{e,t}(k) \to 0$ and it is no longer limited by a BER floor.

In the OS-ASC scheme, the similarity between the detection criterion of d_k and t_k implies that $P_{e,d}(k)$ can also be written as the $P_{e,t}(k)$ expression above. $P_{k|k-1}$ is replaced by $P_{k|k}$ since $\hat{h}_{k|k}$ is passed onto the data channel, not $\hat{h}_{k|k-1}$. Also, SNR_t is replaced by $SNR_d \triangleq \frac{\rho_d^2 \sigma_h^2}{\sigma_w^2}$, which is the data channel SNR.

Except for the error floor removal, OS-ASC provides better channel tracking ability. Let $P^{sup} \triangleq \lim_{k \to \infty} P_{k|k}$ be defined as the steady-state channel estimation MMSE. If the KF converges correctly, $P_{k|k} \approx P_{k-1|k-1}$ as $k \to \infty$. By substituting the expression of K_k in the Kalman gain equation into the Riccatti equation and solving for $P_{k|k}$ as $k \to \infty$, P^{sup} is given by [5]

$$P_{OS-ASC}^{sup} = \frac{\sigma_h^2}{\gamma + \sqrt{\gamma^2 + \frac{a^2}{1-a^2}SNR_t}}. \tag{3}$$

where $\gamma = \frac{1}{2}(1 + SNR_t)$. For superimposed PAT and NS-ASC, P^{sup} is given by the same expression except all the SNR_t's are replaced by β [5]. As $SNR \to \infty$, P^{sup} is lower bounded by $\beta = 1$ for superimposed PAT and NS-ASC, but $P_{OS-ASC}^{sup} \to 0$. Therefore, OS-ASC could provide better tracking ability over the other two superimposed schemes since P_{OS-ASC}^{sup} is unbounded.

V. SIMULATION RESULTS

In this section, simulation results are used to access the applicability of the various CE/DD schemes. The simulation parameters are given by the following: center frequency $f_c = 1.8 \times 10^9$ Hz (High-tier IS-136) [4], symbol period $T = 4.12 \times 10^{-5}$s, symbol/chip pulse = square root raised cosine with 0.35 roll-off, OS-ASC temporal frame length = 162 symbols, $P = 1$, $\eta = 0.1$, $\sigma_h^2 = 1$, and $N = 2$. It is assumed that the power distribution is equal for all symbols, meaning that $\rho_t^2 = \rho_d^2$. The channel coefficients are generated by the method in [7] and 1000 Monte Carlo runs are performed per simulation point.

In order to ensure fair comparisons between the various schemes, two assumptions are made in the simulations. Firstly, all schemes have the same amount of available bandwidth.
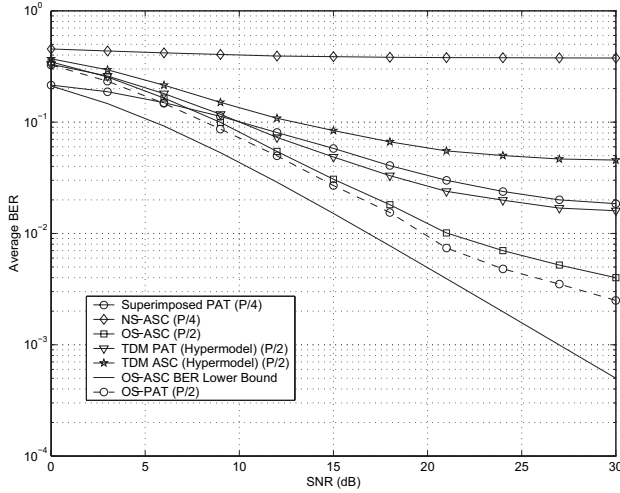
Fig. 3. Average BER versus SNR for $a = 0.95$ and $\eta = 0.1$. For a frame length of 162 symbols, $\eta = 0.1$ means that $10\% = 16$ symbols are pilots / ASC symbols. For a TDM RPP-1 scheme, this translates to 1 pilot / ASC symbol being inserted for every $\lfloor 162/16 \rfloor = 10$ data symbols.

Fig. 4. Average BER versus SNR for various constellations used in OS-ASC with $a = 0.95$ dB and $\eta = 0.1$.

Other schemes that use only half the bandwidth of OS-ASC enjoy the benefit of being able to use the extra bandwidth to transmit at twice the symbol rate of OS-ASC. For example, if each OS-ASC channel has 162 symbols per frame, then TDM schemes would have 324 symbols per frame, and Superimposed PAT and NS-ASC would also have 324 symbols in each channel. The frame's time duration is common for all schemes. This is to ensure that OS-ASC does not have any data rate gains over the other schemes. Secondly, a total power budget of $162P$ is assigned per frame. With equal power distribution, superimposed PAT and NS-ASC symbols have power of $P/4$, while TDM and OS symbols have power of $P/2$. This assumption assures that schemes with more symbols per frame are not biased with having more transmission power per symbol.

Fig. 3 shows the average BER versus SNR with $a = 0.95$ (normalized fading rate $f_D T \approx 0.02$) and $\eta = 0.1$. All symbols are DBPSK encoded and an asymmetric BPSK constellation with points at $\{+1, +j\}$ is chosen to modulate the ASCs [4]. The power allocated to each symbol is marked in parenthesis for each scheme. The high BER floor for NS-ASC is evident in this figure. One interesting observation is that OS-ASC performs better than superimposed PAT, and the performance gap increases as SNR increases. This can be explained intuitively by the derivation in Appendix I. For superimposed PAT, $y'_k = \rho_d d_k \hat{h}_{k|k} + (\rho_t t_k + \rho_d d_k)\tilde{h}_{k|k} + w_k$ whereas for OS-ASC, $y_{tk} = \rho_t t_k \hat{h}_{k|k-1} + \rho_t t_k \tilde{h}_{k|k-1} + \mathbf{s}_t^H \mathbf{w}_k$. Since orthogonal codes do not enhance the AWGN statistics, the superimposed PAT detector has an extra interference term $\rho_d d_k \tilde{h}_{k|k}$ to handle. As SNR increases, w_k becomes less significant and the interference term dominates the performance. If orthogonal codes of length $N = 2$ are similarly applied to superimposed PAT (OS-PAT) to remove interchannel interference, its performance becomes slightly better than OS-ASC. However, OS-PAT transmits only at half the data rate of OS-ASC because its bandwidth is enlarged by the spreading codes and half the symbols in the frame are pilot symbols. Therefore,
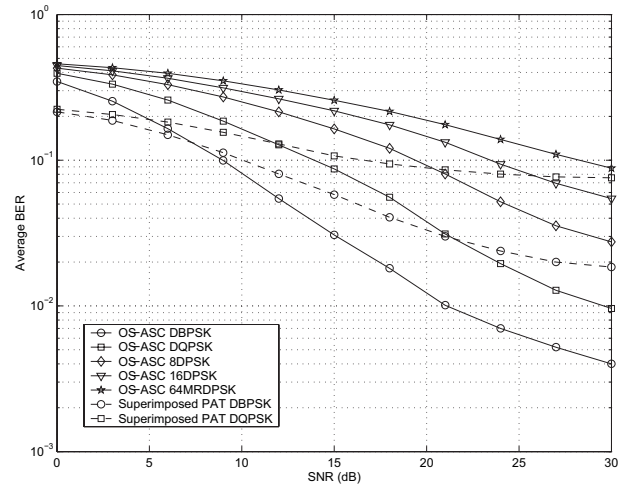
OS-ASC is still preferred over superimposed PAT and OS-PAT when both data transmission rate and BER performance are criteria to be considered.

Since superimposed PAT is compared against the Hyper-model TDM PAT in [5], the TDM schemes in Fig. 3 are simulated using the same TDM PAT receiver model as [5] for proper comparison. Since OS-ASC outperforms superimposed PAT, it also performs better than the two TDM schemes as seen in Fig. 3. Finally, the OS-ASC lower bound is obtained by setting $P_{e,t}(k) \approx P_{e,d}(k)$, $P_{k|k-1} = P_{k|k} = 0$, $\mathcal{K} = 1$, $SNR_t \approx SNR_d = SNR/2$, and $d_{min} = 2$ in (4).

Fig. 4 shows the average BER versus SNR for OS-ASC with higher rate constellations. Two lines of superimposed PAT are also plotted for performance comparison purposes with the corresponding OS-ASC scheme. The OS-ASC subblock structure in the pilot channel is specially constructed for DQPSK, 8DPSK, 16DPSK, and 64MRDPSK. The first two symbols in each subblock are DQPSK symbols to limit the number of parallel KF's required in the receiver. The ASC at the end of each subblock is an asymmetric DQPSK symbol to increase the probability of correct detection and aid the process of breaking isometry [4]. The other symbols in between are modulated by constellations described in the legend of Fig. 4. The data channel consists purely of a continuous stream of data symbols also modulated by constellations described in the legend of Fig. 4. It does not contain any ASCs or special structures.

VI. CONCLUSION

In this letter, the superimposed PAT, NS-ASC, and OS-ASC schemes were studied for PSK signals in a narrowband Rayleigh fading channel modelled by a first-order Gauss-Markov process. The motivation of applying the ASC method in a superimposed framework arises from the observed superior performance of superimposed PAT over TDM PAT in [5]. The NS-ASC scheme encounters a high BER error floor, but the novel OS-ASC scheme eliminates this problem and provides better BER performance over superimposed PAT. When both data transmission rate and BER performance are

important performance criteria, OS-ASC is an attractive alternative to superimposed PAT in the superposition framework.

APPENDIX I
THE DERIVATION OF THE ML DETECTORS

For the detection of d_k in superimposed PAT, y_k in column one of Table I can be rewritten in the form of $y_k = (\rho_t t_k + \rho_d d_k)(\hat{h}_{k|k} + \tilde{h}_{k|k}) + w_k$ where $\tilde{h}_{k|k} = h_k - \hat{h}_{k|k}$ is the channel estimation error. Since the detector for d_k is based on the innovations $y'_k = y_k - \rho_t t_k \hat{h}_{k|k}$, $y'_k = \rho_d d_k \hat{h}_{k|k} + (\rho_t t_k + \rho_d d_k)\tilde{h}_{k|k} + w_k$. Given the pilot symbol t_k, the past observations $\mathbf{y}_1^{k-1} = [y(1), \cdots, y(k-1)]$, and all the past transmitted symbols $\mathbf{d}_1^{k-1} = [d(1), \cdots, d(k-1)]$ detected correctly, y'_k is Gaussian distributed with the following statistics: $E[y'_k | \mathbf{y}_1^{k-1}, t_k, d_k, \mathbf{d}_1^{k-1}] = \rho_d d_k \hat{h}_{k|k}$, and $E[y'_k - \rho_d d_k \hat{h}_{k|k} | \mathbf{y}_1^{k-1}, t_k, d_k, \mathbf{d}_1^{k-1}] = |\rho_t t_k + \rho_d d_k|^2 P_{k|k} + \sigma_w^2$. Given the observation y'_k, the *a posteriori* probability of d_k is

$$P(d_k | y'_k, \mathbf{y}_1^{k-1}, t_k, \mathbf{d}_1^{k-1}) = \frac{[P(y'_k | \mathbf{y}_1^{k-1}, d_k, t_k, \mathbf{d}_1^{k-1}) P(d_k)] P(\mathbf{y}_1^{k-1}, t_k, \mathbf{d}_1^{k-1})}{P(y'_k, \mathbf{y}_1^{k-1}, t_k, \mathbf{d}_1^{k-1})}$$

Thus, given $y'_k, \mathbf{y}_1^{k-1}, t_k$, and $\mathbf{d}_1^{k-1}$, the MAP detector is $\hat{d}_k = \underset{d_k \in D_k}{\arg \max} \{P(y'_k | \mathbf{y}_1^{k-1}, d_k, t_k, \mathbf{d}_1^{k-1}) P(d_k)\}$ where D_k is the constellation for d_k. For PSK constellations, only the numerator of the exponential in $P(y'_k | \mathbf{y}_1^{k-1}, d_k, t_k, \mathbf{d}_1^{k-1})$ matters in deciding $\hat{d}_k$. When each $d_k \in D_k$ is equiprobable, the MAP detector simplifies to the ML detector for d_k in column one of Table I.

For the detection of t_k in NS-ASC, y_k can be rewritten as $y_k = \rho_t t_k (\hat{h}_{k|k-1} + \tilde{h}_{k|k-1}) + v_k$. Using the same procedure as above with y'_k replaced by y_k, $E[y_k | \mathbf{y}_1^{k-1}, t_k, \mathbf{t}_1^{k-1}] = \rho_t t_k \hat{h}_{k|k-1}$, and $E[y_k - \rho_t t_k \hat{h}_{k|k-1} | \mathbf{y}_1^{k-1}, t_k, \mathbf{t}_1^{k-1}] = \rho_t^2 P_{k|k-1} + \sigma_v^2$, we arrive at the ML detector for t_k.

The detection of t_k in OS-ASC is the same as that for t_k in NS-ASC except that y_k is replaced by y_{tk}, v_k is replaced by $\mathbf{s}_t^H \mathbf{w}_k$ and σ_v^2 replaced by σ_w^2. Also, since y_{dk} has the same form as y_{tk} with similar statistics, the derivation above is used again for the detector of d_k in Table I.

APPENDIX II
ERROR PROBABILITY FOR PSK CONSTELLATIONS IN THE PILOT CHANNEL

The probability of error for the NS-ASC scheme can be obtained by rewriting y_k as $y_k = \rho_t t_k (\hat{h}_{k|k-1} + \tilde{h}_{k|k-1}) + v_k$. Given the derivation in Appendix I and that all the past symbols of $\mathbf{t}_1^{k-1} = [t_1, ..., t_{k-1}]$ are detected correctly, the probability of error for one-dimensional constellations is given by

$$P_{e,t}(k) \approx E_{|\hat{h}_{k|k-1}|^2} \left\{ \mathcal{K}.\mathcal{Q}\left(\sqrt{\frac{\rho_t^2 d_{min}^2 |\hat{h}_{k|k-1}|^2}{2(\rho_t^2 P_{k|k-1} + \sigma_v^2)}} \right) \right\}$$

where $\mathcal{K}$ is the average number of nearest neighbors, d_{min} is the minimum distance between adjacent points in a constellation where the average power is normalized to 1, and $\mathcal{Q}(x) = \int_x^\infty \frac{e^{-\frac{t^2}{2}}}{\sqrt{2\pi}} dt, x \geq 0$. $\hat{h}_{k|k-1}$ is a zero mean Gaussian random variable, which means that $|\hat{h}_{k|k-1}|^2$ is exponentially distributed. By using the following result: $\int_0^\infty \mathcal{Q}(\sqrt{x}) \frac{1}{c} e^{-\frac{x}{c}} dx = \frac{1}{2}\left[1 - \sqrt{c/(2+c)}\right]$, and $x \sim exp(c) = \frac{1}{c} e^{-\frac{x}{c}}$, $P_{e,t}(k)$ can be rewritten as

$$P_{e,t}(k) \approx \frac{\mathcal{K}}{2}\left[1 - \sqrt{\frac{1 - \frac{P_{k|k-1}}{\sigma_h^2}}{\left(\frac{4}{d_{min}^2} - 1\right)\frac{P_{k|k-1}}{\sigma_h^2} + \frac{4}{d_{min}^2}\left(\frac{1}{\beta}\right) + 1}}\right] \tag{4}$$

where β is the SINR defined in (2). Since $x \sim exp(c)$, $E[x] = c$ and c can be found by $E[x] = E\left[\frac{\rho_t^2 d_{min}^2 |\hat{h}_{k|k-1}|^2}{2(\rho_t^2 P_{k|k-1} + \sigma_v^2)}\right]$. For two-dimensional constellations, the 2 in the denominator of the $\mathcal{Q}$ function in $P_{e,t}(k)$ is changed to 4 to account for decision regions that involve both the real and imaginary axes instead of only the real axis. By simplifying $P_{e,t}(k)$ to the form in (4), everything in (4) remains the same except that $\frac{4}{d_{min}^2}$ is changed to $\frac{8}{d_{min}^2}$.

For the OS-ASC scheme, y_{tk} can be rewritten as $y_{tk} = \rho_t t_k (\hat{h}_{k|k-1} + \tilde{h}_{k|k-1}) + \mathbf{s}_t^H \mathbf{w}_k$. The only change inside the $\mathcal{Q}$ function in $P_{e,t}(k)$ is that $\rho_t^2 P_{k|k-1} + \sigma_v^2$ becomes $\rho_t^2 P_{k|k-1} + \sigma_w^2$. When this is evaluated to the form in (4), β is replaced by SNR_t.

REFERENCES

[1] P. H. Y. Wu and A. Duel-Hallen, "Multiuser detectors with disjoint Kalman channel estimators for synchronous CDMA mobile radio channels," *IEEE Trans. Commun.*, vol. 48, no. 5, pp. 752–756, May 2000.

[2] L. Lindbom, M. Sternad, and A. Ahlen, "Tracking of time-varying mobile radio channels part I: the Wiener LMS algorithm," *IEEE Trans. Commun.*, vol. 49, no. 12, pp. 2207–2217, Dec. 2001.

[3] H. Zamiri-Jafarian and S. Pasupathy, "Adaptive MLSDE using EM algorithm," *IEEE Trans. Commun.*, vol. 47, no. 8, pp. 1181–1193, Aug. 1999.

[4] S. Lam, K. N. Plataniotis, and S. Pasupathy, "Isometric data sequences and data modulation schemes in fading channels," *IEEE Trans. Commun.*, vol. 52, no. 3, pp. 406–415, Mar. 2004.

[5] M. Dong, L. Tong, and B. M. Sadler, "Optimal insertion of pilot symbols for transmissions over time-varying flat fading channels," *IEEE Trans. Signal Processing*, vol. 52, no. 5, pp. 1403–1418, May 2004.

[6] J. K. Cavers, "An analysis of pilot symbol assisted modulation for Rayleigh fading channels," *IEEE Trans. Veh. Technol.*, vol. 40, no. 4, pp. 686–693, Nov. 1991.

[7] D. J. Young and N. C. Beaulieu, "The generation of correlated Rayleigh random variates by inverse discrete Fourier transform," *IEEE Trans. Commun.*, vol. 48, no. 7, pp. 1114–1127, July 2000.